



ELSEVIER

Available online at [www.sciencedirect.com](http://www.sciencedirect.com)

SCIENCE @ DIRECT®

Applied Surface Science 212–213 (2003) 563–569

applied  
surface science

[www.elsevier.com/locate/apsusc](http://www.elsevier.com/locate/apsusc)

# Electronic structure of transition metal high- $k$ dielectrics: interfacial band offset energies for microelectronic devices

Gerald Lucovsky<sup>\*</sup>, Gilbert B. Rayner Jr., Yu Zhang, Charles C. Fulton, Robert J. Nemanich, Guenther Appel, Harald Ade, Jerry L. Whitten

*Department of Physics, North Carolina State University, Campus Box 8202, Raleigh, NC 27695, USA*

## Abstract

Transition metal silicates,  $(\text{ZrO}_2)_x(\text{SiO}_2)_{1-x}$ , have dielectric constants  $k > 10$  that make them attractive for advanced Si devices. Band offset energies relative to Si are an important factor in determining tunneling leakage current, and internal photoemission. Studies by X-ray photoelectron spectroscopy (XPS), Auger electron spectroscopy (AES) and X-ray absorption spectroscopy (XAS) are combined with ab initio calculations to identify the compositional variation of the band-gap, and valence and conduction band offset energies of Zr silicate alloys with respect to Si. The minimum conduction band offset, due to Zr 4d<sup>\*</sup> states, is shown to be *independent* of alloy composition, while valence band offsets decrease monotonically with increasing ZrO<sub>2</sub> content. The implications of these results for direct tunneling are discussed.

© 2003 Elsevier Science B.V. All rights reserved.

PACS: 71.55.Jv; 75.55.+f; 73.20.At

**Keywords:** Ab initio quantum chemical calculations; Plasma processing; Auger electron spectroscopy; X-ray photoelectron spectroscopy; X-ray absorption spectroscopy; Zirconium silicate alloys; Semiconductor–insulator interfaces

## 1. Introduction

Zr and Hf silicate alloys with 10–40% Zr(Hf)O<sub>2</sub> satisfy many requirements for gate dielectrics in advanced Si devices, including relatively high values of  $k$ ,  $\sim 10$ –13, and good thermal stability to  $\sim 8$ –900 °C [1]. This paper combines our studies using X-ray absorption spectroscopy (XAS), Auger electron spectroscopy (AES) and X-ray photoelectron spectroscopy (XPS), with previously reported studies of photoconductivity (PC) [2] and vacuum ultraviolet photoemission spectroscopy (UPS) [3] to determine for the first

time the *complete* compositional dependence of conduction and valence band offset energies for Zr silicate alloys. These new results are integrated into an empirical model for the direct tunneling that demonstrates that the minimum tunneling current is not obtained at the end-member ZrO<sub>2</sub> with the highest dielectric constant, but rather in  $(\text{ZrO}_2)_x(\text{SiO}_2)_{1-x}$  alloys with  $x < 0.5$ .

## 2. Experimental results

Zr silicate alloys were prepared by remote plasma enhanced chemical vapor deposition (RPECVD) at 300 °C using silane (SiH<sub>4</sub>) as the Si-atom source gas, and Zr *t*-butoxide as the Zr-atom source gas [4]. These

<sup>\*</sup> Corresponding author.

E-mail address: [gerry\\_lucovsky@ncsu.edu](mailto:gerry_lucovsky@ncsu.edu) (G. Lucovsky).

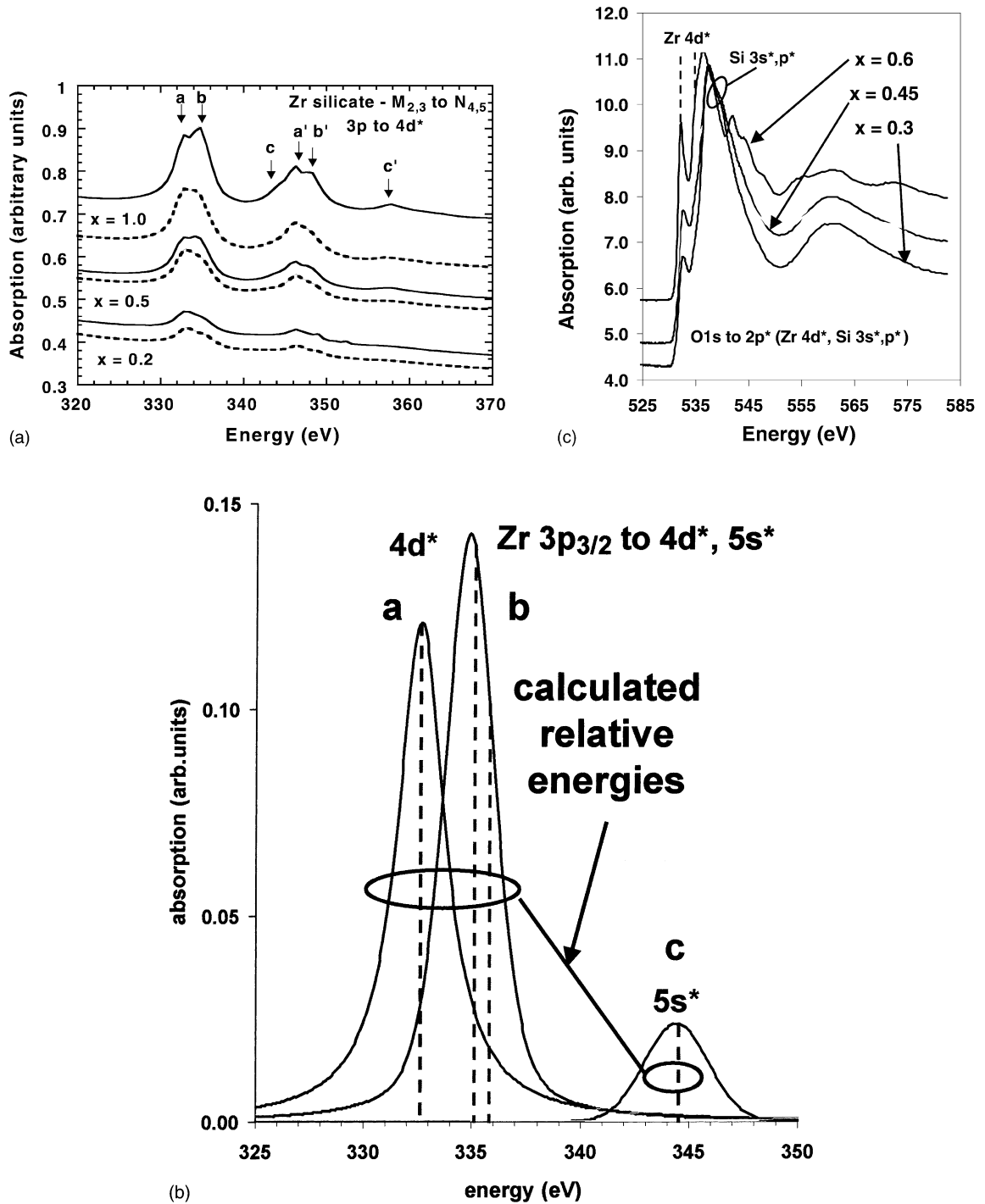


Fig. 1. (a) XAS  $M_{2,3}$  spectra for Zr silicate alloys indicating that features are independent of second neighbor alloy atoms, Si or Zr:  $a$ ,  $b$ ,  $c$  and  $a'$ ,  $b'$ ,  $c'$  designate energy differences between the  $M_2$  and  $M_3$  p-states, respectively, and the anti-bonding Zr-states. Dotted lines are as-deposited and dashed lines are after a 900 °C rapid thermal anneal. (b) Deconvolution of XAS spectrum  $M_{2,3}$  transitions in  $ZrO_2$ . The dashed lines are obtained from ab initio calculations. (c) O  $K_1$  edge spectra for Zr silicate alloys indicating a constant energy difference between the lowest Zr  $4d^*$  state, and the edge corresponding to Si  $3s^*$  transitions.

were injected downstream from a remote  $O_2/He$  plasma, and excited O-species extracted from that plasma were used to initiate the remote plasma deposition process. The deposited alloys are fully oxidized with no detectable Si–Zr bonding as determined from analysis of on-line AES. Similar results have also been obtained for Hf silicate alloys by RPECVD. Alloy compositions were determined by Rutherford backscattering (RBS), and these were used to calibrate on-line AES where a linear dependence

was demonstrated between the ratio of the derivative spectrum peak to peak heights for  $Zr_{M_{VV}}$  and  $O_{K_{VV}}$  features and the RBS determined compositions. This article summarizes the results of XAS, XPS and AES as applied to determination of band offset energies relative to the conduction and valence band edges of crystalline Si.

XAS studies of  $M_{2,3}$  to  $N_{4,5}$ ,  $O_1$  and  $O_{2,3}$  ( $3p_{1/2}$ ,  $3p_{3/2}$  to  $4d^*$ ,  $5s^*$  and  $5p^*$ ) transitions in Fig. 1a have established that relative energies of localized  $4d^*$  states do

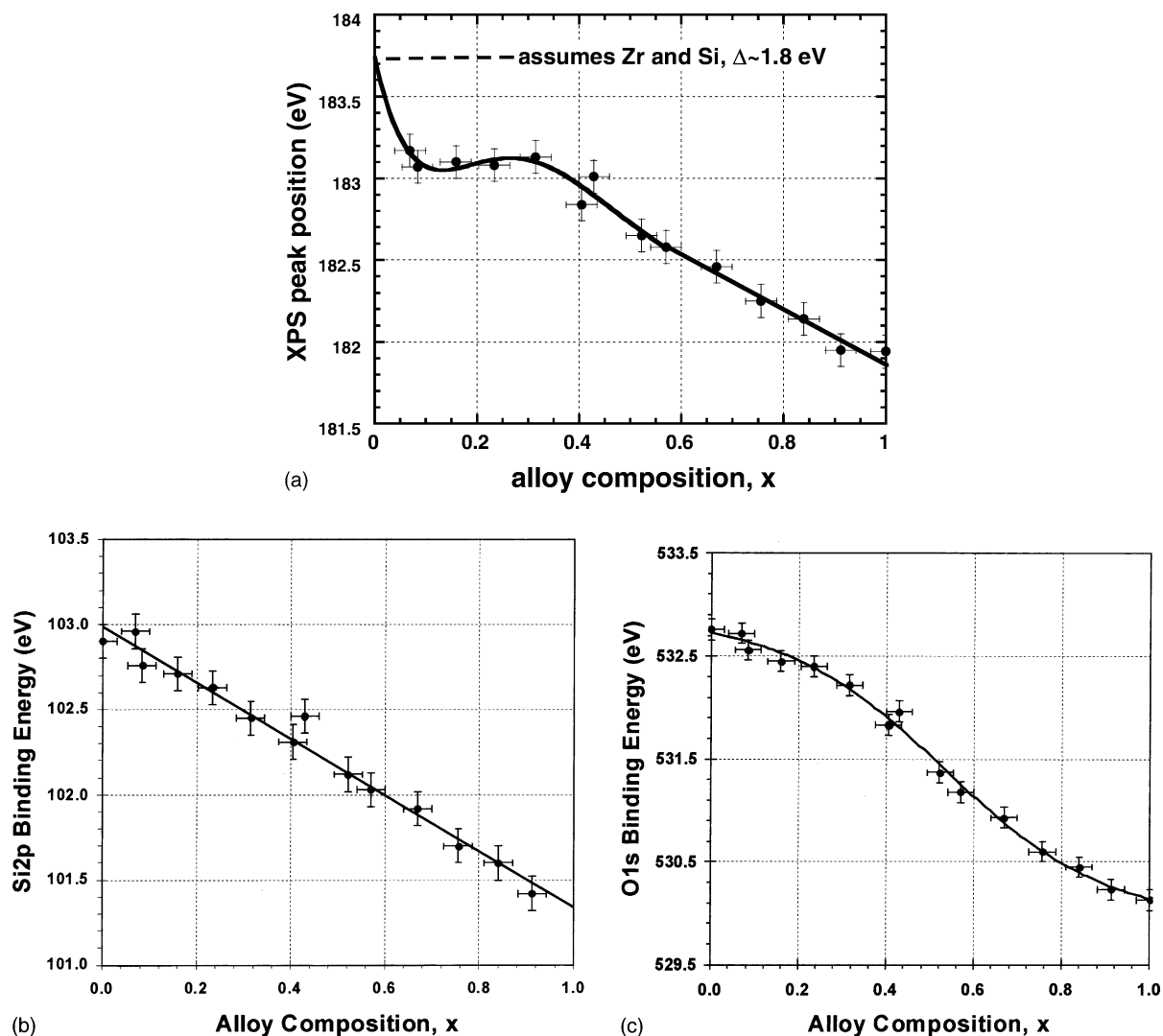
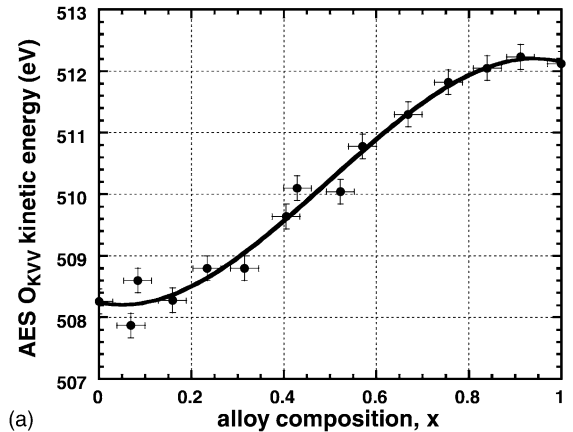


Fig. 2. XPS chemical shifts of (a) Zr  $3d_{5/2}$ ; (b) Si  $3p$ ; and (c) O  $1s$  core levels from as-deposited Zr silicate alloys as a function of alloy composition  $x$ . The solid lines in (b) and (c) are expected on the basis of electronegativity equalization, as is the equal total shifts of the Si  $3p$ , and extrapolated Zr  $3d_{5/2}$  dependence.

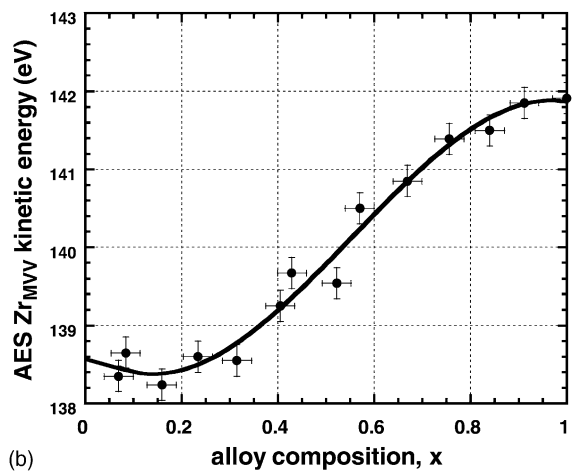
not change with alloy composition  $x$  (Si or Zr second neighbors), or with the degree of crystallinity [5], confirming predictions of ab initio theory. Results in Fig. 1b demonstrate excellent agreement between ab initio theory calculations as small clusters, and confirm that the two features in the  $M_{2,3}$  spectra of Fig. 1a are transitions that terminate in anti-bonding  $4d^*$  states and the third feature is associated with  $5s^*$  states. More importantly, studies of O-atom  $K_1$  transitions in Fig. 1c for silicate alloys indicate that the energy difference between the Zr  $4d^*$  states that mix with O  $2p^*$  states and contribute to lowest conduction band structure, and the Si  $3s^*$  states that mix and contribute to the next conduction are independent of the alloy composition.

The binding energies of Zr  $3d_{5/2}$ , Si  $2p$  and O  $1s$  core states were derived from XPS and display different degrees of non-linearity when plotted as a function of the alloy composition  $x$  [4]. The binding energies of each of these core states shift to more negative values with increasing  $x$ , consistent with the predictions of model calculations based on the relative atomic electronegativities [4]. More importantly, the non-linearities in the compositional dependence for low alloy compositions,  $x \sim 0.1$ – $0.3$ , in Fig. 2a–c, respectively, for the Zr  $3d_{5/2}$ , Si  $2p$  and O  $1s$  transitions, are consistent with a bonding model for the introduction of  $ZrO_2$  into  $SiO_2$ , in which four Zr–O ionic bonds are formed by break-up (or *disruption*) of the covalent network, and four donor–acceptor electrostatic pair bonds are formed between non-bonding pairs on network O-atoms and the  $Zr^{4+}$  ions. As  $x$  is increased, these electrostatic bonds are replaced by additional Zr–O ionic bonds while maintaining an effective coordination of eight. This replacement is complete when the alloy composition reaches  $x \sim 0.5$ , and the compositional dependencies show significantly reduced non-linearities for  $x$  between 0.5 and 1.0 ( $ZrO_2$ ).

The kinetic energies of  $Zr_{MNV}$  and  $O_{KVV}$  AES electrons, displayed in Fig. 3a and b, show a non-linear compositional dependence significantly different from that observed in XPS [4]. A comparison between XPS binding energies, and the AES results based on the calculation of [6], indicates that the sigmoidal dependencies of the AES features reflect a markedly non-linear behavior in the energies of the highest valence band states with respect to vacuum. This is consistent with ab initio calculations as well.



(a)



(b)

Fig. 3. AES chemical shifts of (a)  $O_{KVV}$  and (b)  $Zr_{MNV}$  kinetic energies in as-deposited Zr silicate alloys as a function of composition. The plots in (a) and (b) are for the *highest energy peaks* in the respective AES spectra. The solid lines are polynomial fits that are intended to emphasize the sigmoidal character of the compositional dependence.

### 3. Data analysis

The  $O_{KVV}$  transition in  $\alpha$ - $SiO_2$  has been investigated theoretically, and it has been demonstrated that the highest AES kinetic energy is associated with two electrons being released from the non-bonding O  $2p$   $\pi$  states at top of the valence band; one of these is the emitted AES electron, and the second fills the O  $1s$  core hole formed by electron beam excitation [6]. Based on this mechanism, and combined with the

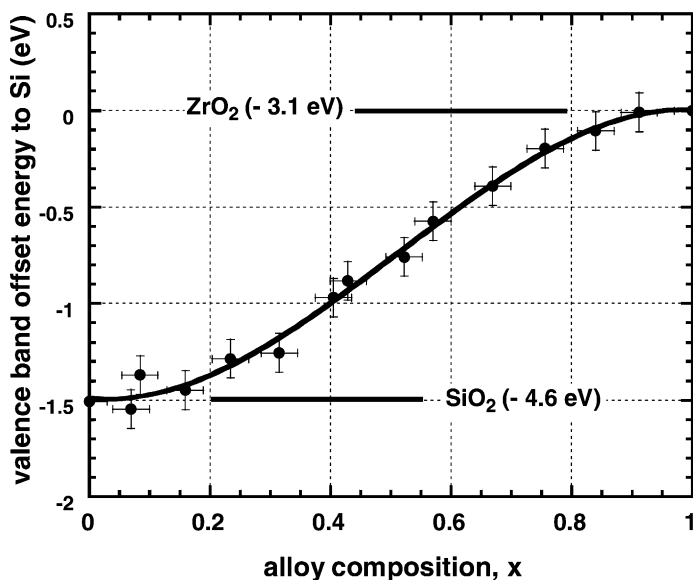


Fig. 4. Calculated values of the valence band offset energies relative the valence band of crystalline Si at approximately  $-5.2$  eV as calculated from the two parameter empirical model of Eq. (1). The plot in is derived from O-atom XPS and AES data. The sigmoidal dependence is due to differences between the compositional dependencies of the respective XPS and AES results used as input, and not on empirical constants.

XPS and AES results of this study, a model has been developed in Eq. (1) that provides an estimate of the valence band offsets of the Zr silicate alloys with Si as a function of composition  $x$ . This model assumes that a core hole in the O-atom 1s state is filled by an electron

from the top of the valence band, and that the Auger electron is also emitted from the top of the valence band as well.  $E_{BE}(O\ 1s)$  is the magnitude of the XPS binding energy, and  $E_{KE}(O_{KVV})$  is the average kinetic energy of the Auger electron with respect to the top of

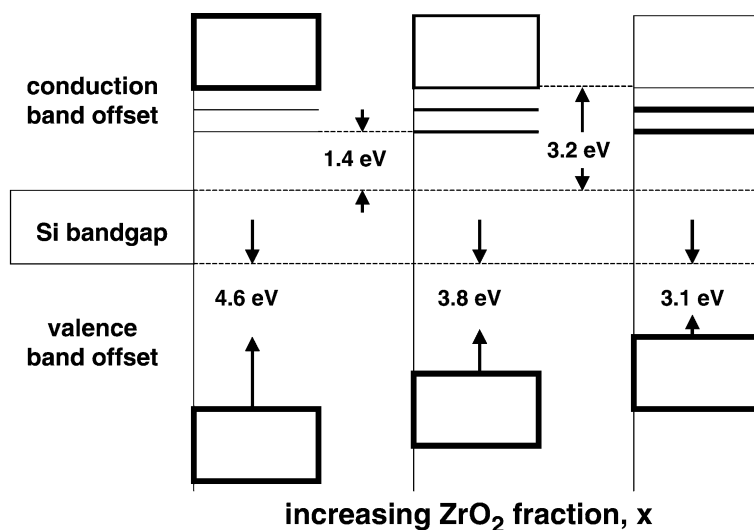


Fig. 5. Schematic representation of conduction and valence band offset energies as function of increasing  $x$ .

the valence band edge. Under these conditions

$$V_{\text{offset}}(x) \sim -0.5A[E_{\text{BE}}(\text{O } 1s) - E_{\text{KE}}(\text{O}_{\text{KVV}})] + B \quad (1)$$

where  $A$  and  $B$  are constants, 0.44 and 1.2, respectively, that adjust the respective values of  $V_{\text{offset}}(0)$  and  $V_{\text{offset}}(1)$  to 4.6 eV for  $\text{SiO}_2$  and 3.1 eV for  $\text{ZrO}_2$  [7,8]. This model is presented in Fig. 4, and the sigmoidal shape of the polynomial fit in Fig. 4 is determined by the relative compositional dependencies of the XPS (O 1s) and AES ( $\text{O}_{\text{KVV}}$ ) data in Figs. 2a and 3a, respectively. The analysis has also been applied to the  $\text{Zr}_{\text{MNV}}$  AES and Zr 3d XPS results of Figs. 2b and 3b, respectively, and gives essentially the same compositional dependence for valence band offset energies as is displayed in Fig. 4, but with different empirical constants,  $A'$  and  $B'$ .

Fig. 5 includes a schematic representation of the conduction and valence band offset energies of Zr silicate alloys as function of alloy content. This schematic combines the XAS results of Fig. 1 with the model of Eq. (1). The ab initio calculations have established that the O  $\text{K}_1$  XAS final states are essentially the same as the calculated conduction band states from band-gap excitations. This means that all of the band-gap variation occurs in the valence band offsets, so that the offset energies of both the Zr  $4d^*$  states and Si  $3s^*$  states are constant with respect to the conduction band edge of Si. The contributions of these Zr and Si to the conduction band density of states are proportional to their alloy concentrations, and these states play an important role in determining the direct tunneling current.

#### 4. Conclusions

The combination of experimental results described above, and ab initio theory allow the following conclusions to be made:

- (i) localization of Zr and (other also groups III–V transitional metal) d-states explains the absence of any dependence of  $M_{2,3}$  to  $N_{4,5}$ ,  $O_1$  and  $O_{2,3}$  transition energies on Si alloy content, or crystallinity;
- (ii) non-linear behaviors of the Zr  $3d_{5/2}$ , Si 2p and O 1s binding energies for  $x < 0.5$  are consistent with bonding in a Zr-atom disrupted network in which donor–acceptor pair electrostatic bonds contribute only at low  $x$  [4];
- (iii) the relative degrees of non-linear behaviors for Zr  $3d_{5/2}$  and O 2p confirm the microscopic origin of the enhanced dielectric constants reported for low concentration Zr (and Hf) silicate alloys [7];
- (iv) non-linear behaviors of the  $\text{O}_{\text{KVV}}$  and  $\text{Zr}_{\text{MNV}}$  AES kinetic energies reflect changes in the energy of the top of the O 2p non-bonding valence band states with respect to vacuum, and therefore also reflect changes in band offset energies between the silicate alloy and Si valence band as well;
- (v) the combination of XPS and AES establish that (a) the band-gaps of Zr(Hf) silicate alloys decreases monotonically, but non-linearly between those of  $\text{SiO}_2$  ( $\sim 9$  eV) and  $\text{ZrO}_2$  ( $\sim 5.5$  eV); and (b) that conduction band offset energies associated with the lowest Zr and Si anti-bonding states, and are essentially independent of alloy composition, but that the valence band offsets decrease monotonically with increasing O-atom coordination  $N$ : from  $\sim 4.6$  eV in  $\text{SiO}_2$  ( $N = 2$ ) to 3.7 eV in the stoichiometric silicate,  $x = 0.5$  ( $N = 3$ ), and to 3.1 eV in  $\text{ZrO}_2$  ( $N = 4$ );
- (vi) comparisons between XAS, XPS, AES, PC, internal photoemission (IPE) [2], and optical absorption establish strong final state effects; and
- (vii) the connection between these spectroscopic results and effective tunneling barriers in metal-oxide-semiconductor structures remains as yet unanswered.

If it is assumed that tunneling barriers are correlated with either photoconductive or IPE band-gaps [2], then analysis of tunneling in terms of empirical models developed for  $\text{SiO}_2$  yields an *unrealistically low* electron mass,  $\sim 0.2m_0$  [8]. It is proposed here that the increased current defined by this mass parameter results from tunneling transitions that couple strongly to localized Zr(Hf) anti-bonding  $d^*$  states at the bottom of the conduction band.

The tunneling current displays a minimum value in  $(\text{SiO}_2)_{1-x}(\text{Si}_3\text{N}_4)_x$  pseudo-binary alloy system at  $x \sim 0.5$ , rather than at the end-member  $\text{Si}_3\text{N}_4$  composition which corresponded to the highest  $k$ ,  $\sim 7.6$ , and physically-thickest film for a given equivalent oxide thickness referenced to  $\text{SiO}_2$ . This has been correlated with a linear scaling of the effective barrier height, tunneling mass, and dielectric constant with alloy

content [9]. Using an empirical model for Zr(Hf) silicates, scaled to appropriate offset energies and masses, also gives a non-linear behavior in the direct tunneling current with a minimum at  $x \sim 0.4$ – $0.5$ . Values of the direct tunneling current for  $x = 0.0$  ( $\text{SiO}_2$ ),  $x \sim 0.2$ – $0.3$ , and  $x \simeq 1$  ( $\text{HfO}_2/\text{ZrO}_2$ ) suggest that this dependence is obeyed experimentally. This model does not take into account an enhancement of the dielectric constant for low values of  $x$ ,  $\sim 0.1$ – $0.3$ , which would lead to additional decreases in the tunneling current in that composition region [7]. Combined with high thermal stability and reduced interfacial fixed charge, low Zr(Hf) $\text{O}_2$  content alloys emerge as a strong candidates for advanced devices.

### Acknowledgements

This research is supported by the ONR, AFOSR, SRC and i-Sematech/SRC Front End Processes Center.

### References

- [1] G. Wilk, R.W. Wallace, J.M. Anthony, *J. Appl. Phys.* 89 (2001) 5243.
- [2] V.V. Afanas'ev, A. Stesmans, G.J. Andriaenssens, M.M. Heyns, *Microelectronic Eng.* 59 (2001) 335.
- [3] S. Miyazaki, M. Narasaki, M. Ogasawaga, M. Hirose, *Microelectronic Eng.* 59 (2001) 373.
- [4] G.B. Rayner Jr., D. Kang, Y. Zhang, G. Lucovsky, *J. Vac. Sci. Technol. B*20 (2002) 1748.
- [5] G. Lucovsky, G.B. Rayner Jr., D. Kang, G. Appel, R.S. Johnson, Y. Zhang, D.E. Sayers, H. Ade, J.L. Whitten, *Appl. Phys. Lett.* 79 (2001) 1775.
- [6] D.E. Ramaker, J.S. Murday, N.H. Turner, in: S.T. Pantelides (Ed.), *The Physics of  $\text{SiO}_2$  and its Interfaces*, Pergamon Press, New York, 1978, p. 99.
- [7] G. Lucovsky, G.B. Rayner Jr., *Appl. Phys. Lett.* 77 (2000) 2912.
- [8] W. Zhu, T.P. Ma, T. Tamagawa, J. Kim, R. Carruthers, M. Gibson, T. Furukawa, *IEDM Digest of Technical Papers*, 2001, p. 463.
- [9] G. Lucovsky, Y. Wu, H. Niimi, *J. Vac. Sci. Technol. A* 18 (2000) 1163.